6. DISCUSSION OF EXPERIMENT AND THEORY: HEAT TRANSFER

6.1 Available Data and Correlations for Two-Phase Systems

Heat transfer in air-water system has been widely investigated and serves as an important basis for assessing the relative accuracies of different measurements. All the available data along with smoothed values [83] are displayed in Fig. 6.1. Curve 1 represents the data of Kolbel et al. [84] taken in columns of diameter 19.2 and 29.2 cm fitted with a porous plate distributor and a cylindrical heater of length and diameter 10 cm and 3 cm respectively at 313 K for air velocities in the range 0.0035-1.10 m/s. The present data are in good agreement with their values except for air velocities smaller than about 0.025 m/s. Fair et al. [85] data at 300 K in a 0.457 m diameter column, referring to column wall and air-water dispersion, are shown as curve 2 in Fig. 6.1. Stationary baffles comprised of perforated plates with holes of varying diameters and spacing were placed in the column and water flow of 10 to 13 gallons per minute was maintained. When the baffles were given a reciprocating rapid motion (1050 cycles per minute), heat transfer coefficient values were consistently higher than those shown in Fig. 6.1. Data were also obtained for a 1.07 m diameter column fitted with forty-two tubes of 0.038 m diameter in two concentric circles of diameters 0.98 and 0.88 m. One of the tubes of the bundle served as a heater. Their graphical plot of heat transfer coefficient values showed an appreciable scatter but there was an overall general agreement in the two sets of experimental values which they have represented by simple correlation. They point out a greater uncertainty in their low air velocity data. From Fig. 6.1, it is clear that their data are consistently greater than the present data, the disagreement is about 20% at lower air velocities and it decreases to about 5% at higher air velocities. At least part of this systematic disagreement may be attributed to the liquid flow and presence of baffles in the heat transfer rates for the column wall and an immersed surface.

Burkel's data [86, 87] referring to an immersed surface (coil) in a 0.19 m cylindrical column are shown as set 3 in Fig. 6.1. At higher air velocities his data are differing by about 10% from the present work and this difference is about 15%

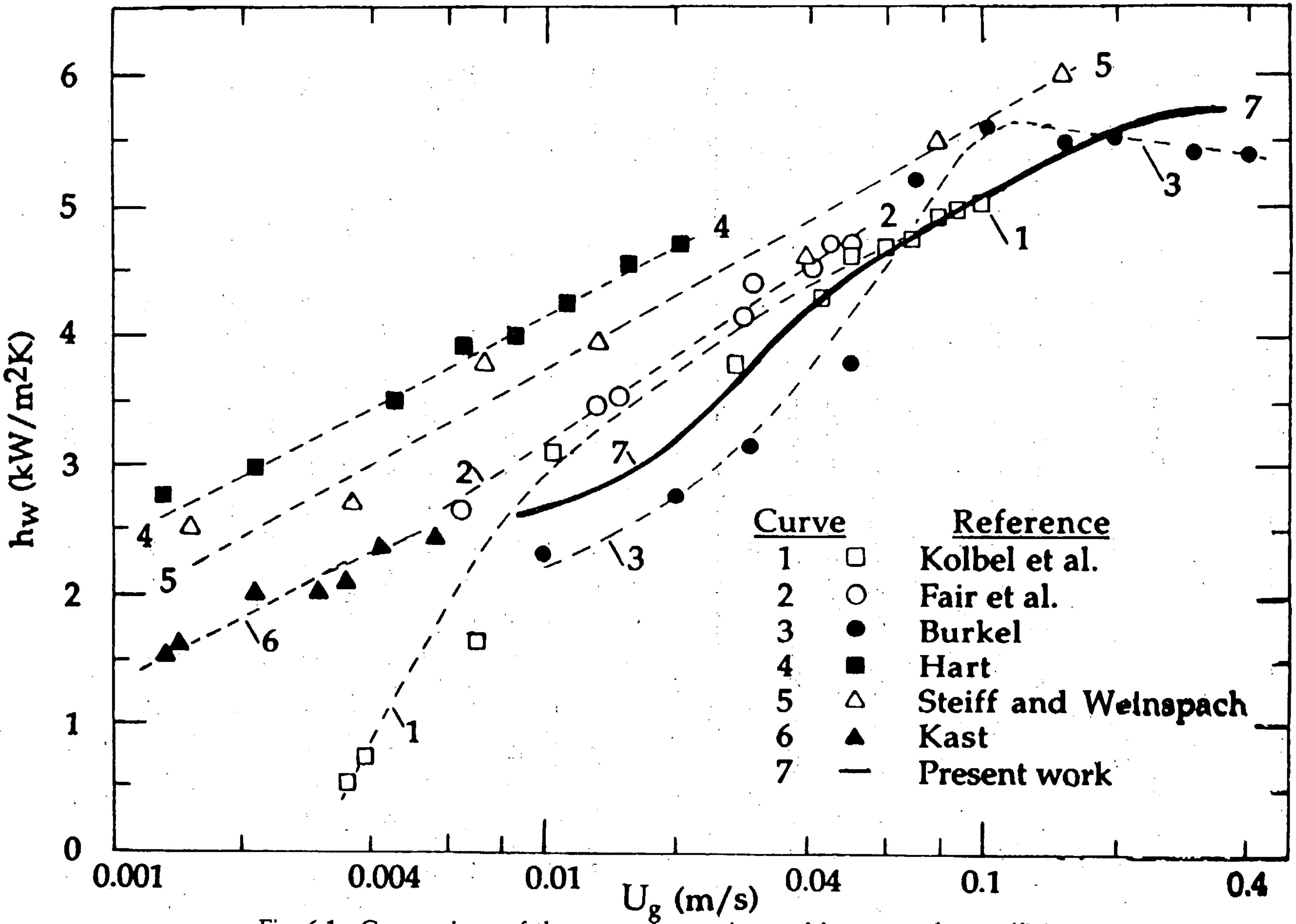

Fig. 6.1. Comparison of the present experimental heat transfer coefficient values with the measurements of other workers for the air-water system as a function of superficial air velocity and temperatures in the range 300-344 K.

at lower air velocities. His values are considered unreliable on the whole in view of their general disagreement from all the available data sets, and their qualitative trend of variation with air velocity. Set 4 of Fig. 6.1 refers to the data of Hart [88] at 344 K taken in a column of 9.9 cm diameter and equipped with a single nozzle of 6.35 mm diameter. Water was allowed to flow with a constant velocity, and column wall to air-water dispersion heat transfer coefficient was measured. The apparent disagreement of these data from present work is due to a higher temperature to which these refer. Hart [88] has empirically correlated his data to show their general agreement with the data of set 2. This will imply that these data [88] like set 2 are consistently greater than sets 1 and 7. Further, this disagreement increases with decrease in air velocity.

Steiff and Weinspach [89] employed a 19 cm diameter column fitted with a sintered plate distributor and measured heat transfer coefficient between the heated column wall and the air-water dispersion at 313 K. The latter was obtained by the cocurrent flow of air and water through the column. These data, Set 5, are consistently greater than all the other data sets. The disagreement with set 7 is 40% at the lowest air velocity and decreases to 10% at the highest air velocity. This disagreement if not attributed to the difference between the measured column wall and an immersed surface heat transfer coefficient in view of the above discussion, then it would suggest that the way these workers have averaged their heated surface temperature and column water temperature might have given rise to systematic error in their computed heat transfer coeffcient values. The inference that these data are not reliable is, however, more conclusive and evident from the analysis of Fig. 6.1.

Kast [80] has reported heat transfer coefficient for 28.8 cm diameter column wall and air-water dispersion as a function of air velocity in the range 0.02 to 0.6 cm/s. His data shown as set 6 in Fig. 6.1, appear to be consistent with the data of Fair et al. [85] (set 2) and probably with Hart [88] (set 4), but are systematically smaller than Steiff and Weinspach [89] (set 5) and greater than Kolbel et al. [84] (set 1).. However, for U_g smaller than 0.008 m/s, the bubble induced liquid mixing in the column is sensitive to the column diameter and the nature of the air sparger. As a result one could expect significant differences in the heat transfer values measured for the column wall for an immersed surface. We think that this is the reason for appreciable differences in the heat transfer rate values reported by different workers in this low air velocity region shown in Fig. 6.1.

The heat Transfer coefficient values obtained as a function of air velocity in the present work and shown in Fig. 6.2 by curve are compared with the predictions of various available correlations and models. Fair et al. [85] on the basis of their data in the air velocity range 0.023 to 0.107 m/s proposed the following empirical correlation:

$$h_w = 8849\ U_g^{0.22} \qquad 6.1$$

The expressions leads to values, curve b in Fig. 6.2 that are in poor agreement with our measured values both at low and high gas velocities . Further, this form for h_w is incapable of reproducing the qualitative feature of heat transfer coefficient according to which h_w approaches a constant value at higher velocities.

Mersmann [91] proposed a correlation for the heat transfer in bubble columns in analogy to the phenomenon of free convection by replacing the Grashof number with the Archimedes number. His [91] final result is

$$h_w = 0.107\ k_L \left(g/v_L \alpha\right)^{1/3} Pr^{0.226} \qquad 6.2$$

Computed values of h_w at 308 K from Eq. (6.2) is 4.21 kW/m^{2}K is independent of air velocity. The constant h_w value which is invariant with respect to air velocity on the basis of our data is 5.8 kW/m^{2}K. Thus, it is clear that Mersmann [91] theory predictions are appreciably smaller than the measured values.

Zehner [92] heat transfer model assumes a thinned thermal boundary layer on the heat transfer surface when bubbles are present. The length of the boundary layer was taken to be the same as the distance between successive bubbles, l, and its values was assumed to be constant as 7 mm. The heat transfer through the boundary layer is described as that over a flat heated plate. His final expression for gas velocities up to about 0.1m/s is

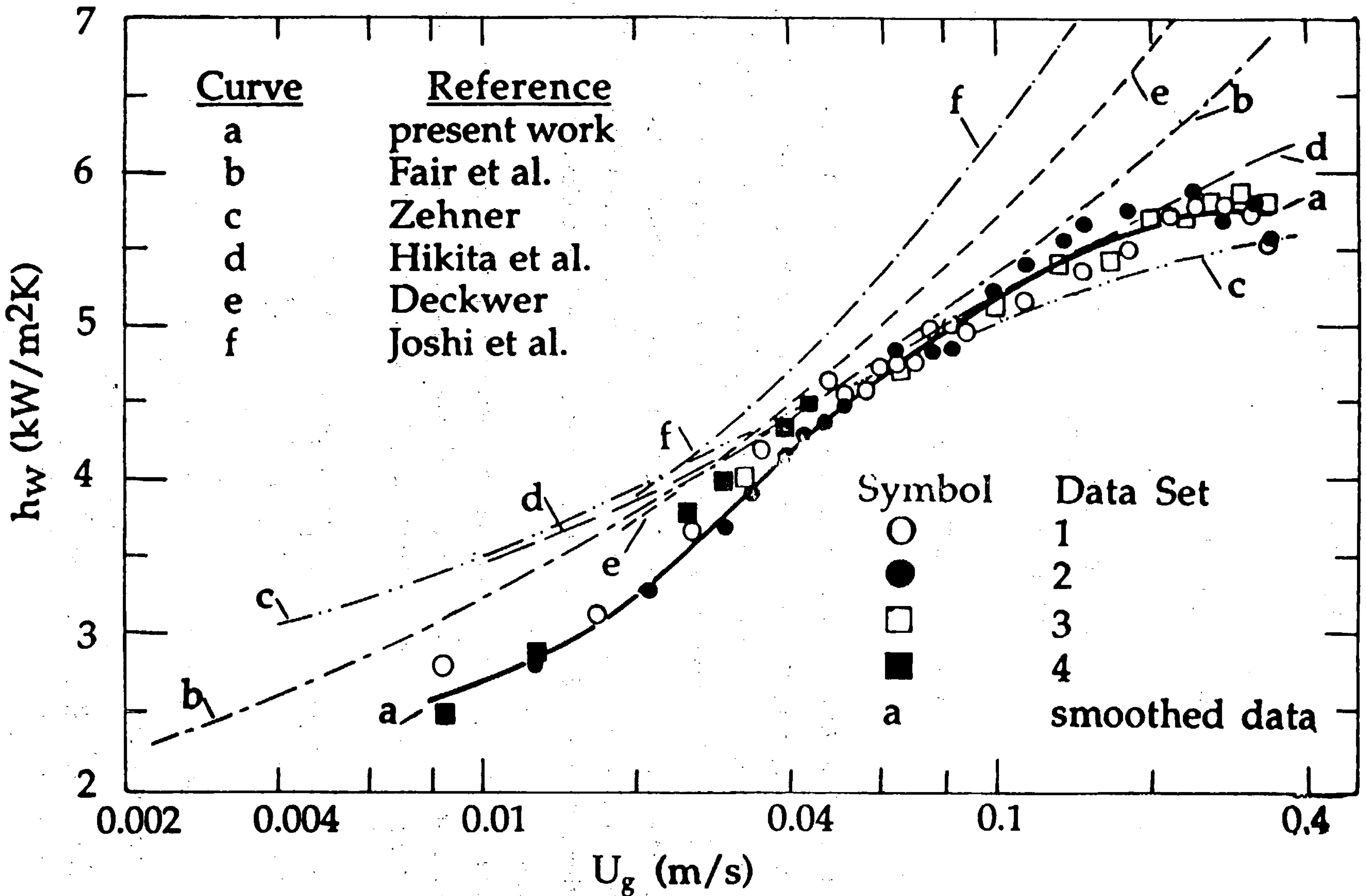

Fig. 6.2. Comparison of experimental heat transfer coefficient with various computed sets for air-water system as a function of superficial air velocity at 309 K.

$$h_w = 0.18\left(1 - \epsilon_g\right)\left[k_L^2\ \rho_L^2\ C_{pL}\ V_F^2 / l\ \ \mu_L\right]^{1/3} \tag{6.3}$$

Where

$$l = d_b\left(\pi / 6\epsilon_g\right)^{1/3} \tag{6.4}$$

$$V_F = \left[\frac{1}{2.5}\left(\frac{\rho_L - \rho_g}{\rho_L}\right) g\, D_C\, U_g\right]^{1/3} \tag{6.5}$$

and

$$\epsilon_g = U_g\ /\ \left[0.25 \exp\left(5\ \epsilon_g\right)\right] \tag{6.6}$$

Computed values from these relations are shown as set C in Fig. 6.2. In the lower air velocity range (<0.06 m/s), his values are greater than our measured values, but are in good agreement for the range 0.06 to 0.10 m/s. At higher velocities his values approach to a constant value for heat transfer coefficient which, however, is smaller than the experimentally obtained values. The difference is about 8 percent. One important factor to note in this theory is that h_w is dependent on column diameter. Several workers have claimed h_w to be independent of column diameter.

Hikita et al [87] proposed the following empirical correlation based on their data for several liquids having widely different values of viscosity and surface tension for temperatures (295 to 318 K) and air velocities (5.3 to 34 cm/s):

$$\frac{h_w}{\rho_L\ C_{pL}\ U_g}\left(\frac{C_{pL}\ \mu_L}{k_L}\right)^{2/3} = 0.411\left(\frac{U_g\ \mu_L}{\sigma_L}\right)^{-0.851}\left(\frac{\mu_L g}{\rho_L\ \sigma_L^3}\right)^{0.308} \tag{6.7}$$

They also show that if the influence of σ_L on h_w is ignored, the above relation can be simplified to:

$$\frac{h_w}{\rho_L\ C_{pL}\ U_g}\left(\frac{C_{pL}\ \mu_L}{k_L}\right)^{2/3} = 0.268\left(\frac{U_g^3\ \rho_L}{\mu_L g}\right)^{-0.303} \tag{6.8}$$

Alternatively

$$St = 0.268\left[Re_b\ Fr\ Pr^{2.16}\right]^{-0.303} \qquad 6.9$$

The computed values of h_w form Eq. (6.7) are consistently greater than the experimental values over the entire air velocity range by about 60%. The reason for this large discrepancy lies in the fact that these workers [87] have used their own data in the development of Eq. (6.7). Their data are much higher than the experimental values found by other workers and it could be due to the small size of the heater they have used on the column wall. We adjusted the numerical constant in Eq. (6.7) on the basis of our data to obtain the following relation:

$$\frac{h_w}{\rho_L\ C_{pL}\ U_g}\left(\frac{C_{pL}\ \mu_L}{k_L}\right)^{2/3} = 0.271\left(\frac{U_g\ \mu_L}{\sigma_L}\right)^{-0.851}\left(\frac{\mu_L\,g}{\rho_L\ \sigma_L^3}\right)^{0.308} \qquad 6.10$$

Computed values of Eq. (6.10) are shown in Fig. 6.2 as set d. The data are poorly reproduced in the low as well as in the high gas velocity range.

Kast [90] and many other workers [86-89, 93-96] after him have proposed the calculation of h_w based on an expression of the following general form:

$$St = C_1\left[Re_b\ Fr\ Pr^{C_2}\right]^{-C_3} \qquad 6.11$$

Different values of C_1, C_2 and C_3 have been recommended. A critical study of Deckwer [93] show that a good compromised choice is,

$$St = 0.1\left[Re_b\ Fr\ Pr^2\right]^{-0.25} \qquad 6.12$$

when gas velocity is less than 10 cm/s. Computed values of h_w are shown as curve e in Fig. 6.2. The calculated values are consistently greater than the experimental values, the disagreement increases from 8% at 0.03 m/s to 19% at 0.20 m/s. The form of Eq. (6.12) also does not lead to values which approach to a constant h_w at higher gas velocities.

Joshi and Sharma [97] in contrast to Deckwer [93] have argued that the input gas energy is dissipated and consumed mostly in the wakes of the bubbles and only less than 10% is used to create liquid motion in the bubbly flow regime. Assuming ideal inviscid flow behavior and the presence of multiple interacting cells in the axial direction, they have derived the following expression for the average liquid circulation velocity in the bubble column:

$$V_c = 1.31 \left[g D_C \left(U_g - \epsilon_g U_{b\infty} \right) \right]^{1/3} \tag{6.13}$$

The average axial component of this liquid velocity is:

$$V_a = 1.18 \left[g D_C \left(U_g - \epsilon_g U_{b\infty} \right) \right]^{1/3} \tag{6.14}$$

Substituting this value of V_a in the Sieder and Tate equation, Joshi et al [98] proposed the following relation for the calculation of h_w

$$\frac{h_w D_C}{k_L} = 0.031 \left[\frac{D_C^{1.33} g^{1/3} \left(U_g - \epsilon_g U_{b\infty} \right)^{1/3} \rho_L}{\mu_L} \right]^{1/3} \left(\frac{C_{pL} \mu_L}{k_L} \right)^{\frac{1}{3}} \left(\frac{\mu_L}{\mu_w} \right)^{0.14} \tag{6.15}$$

as shown in Fig. 6.2, computed values based on this relation, curve f, are consistently and significantly greater than the experimental values.

6.2 Available Data and Correlations for Three-Phase Systems

Smith et al. [99] have presented an extensive tabulation of existing correlations for three-phase reactors of column wall or immersed surface to a three-phase dispersion. However, here we will discuss only those correlations and models which are appropriate to mimic the operation of a slurry bubble column in which the continuous liquid phase is either stagnant or moving rather slowly and the turbulent mixing and solids dispersion is caused by the gas bubbling through the column.

Kolbel et al. [100] have measured the heat transfer between a heated probe immersed in water with sand particles and air bubbling up to a maximum velocity of about 12 cm/s. Samples of sand were used with average particle diameter (d_p) as 0.04, 0.075, 0.11 and 0.2 mm. Based on these data, it was proposed that for laminar flow

$$Nu = 222.8\, Re^{0.16} (d_p/d_o)^{0.05} \tag{6.16}$$

and for turbulent flow,

$$Nu = 350.8\, Re^{0.108} (d_p/d_o)^{0.05} \tag{6.17}$$

These correlations were recommended for

$$1 < (d_p/d_o) < 5 \tag{6.18}$$

with $d_o = 0.04$ mm.

Further, Nu and Re are defined as [101]

$$Nu = h_w d_p/k_L \tag{6.19}$$

and

$$Re = U_g \rho_g d_p/\mu_g \tag{6.20}$$

For the present system and operating conditions, the correlation of Eq. (6.17) is applicable. However, the calculations yielded much greater values than the corresponding experimental values. In view of the involvement of d_p and d_o in the correlation, we consider it only of historical importance and do not use it for detailed calculations and comparison with our experimental data in this work. Further, some ambiguity exists about the calculation of Nu and Re, and these are also defined in terms of the diameter of the heating element in one of their works [102].

For two-phase bubble and droplet columns, Mersmann et al. [103, 91] have recommended that the maximum heat transfer coefficient, $h_{w\ max}$, is given by

$$h_{w\ max} = 0.12\left(\frac{g^2\rho_L}{\mu_L}\right)^{\frac{1}{6}}\left(\frac{\rho_L-\rho_g}{\rho_L}\right)^{\frac{1}{3}}\left(k_L\rho_L C_{pL}\right)^{\frac{1}{2}} \qquad 6.21$$

Here all quantities are in SI unit system. For the applicability of this relation, the following condition must also be satisfied.

$$Ar \cdot Pr > 10^6 \qquad 6.22$$

where

$$Ar = \frac{d_b^3(\rho_L - \rho_g)\,g\rho_L}{\mu_L^2} \qquad 6.23$$

and

$$Pr = \frac{\mu_L C_{pL}}{k_L} \qquad 6.24$$

For air-water system in the churn turbulent regime, the product of Ar and Pr is 3.3 x 10^7 for d_b = 7 mm [104, 77]. This validates the applicability of the above correlation to the present work. Calculations revealed that the value of $h_{w\ max}$ is about 4.43 kW/m^{2}K. Our measurements give a value of about 6.2 kW/m^{2}K.

For three-phase systems it is being proposed [105] to examine the validity of this correlation in the following revised form:

$$h_{w\ max} = 0.12\left(\frac{g^2\bar{\rho}}{\bar{\mu}}\right)^{\frac{1}{6}}\left(\frac{\bar{\rho}-\rho_g}{\bar{\rho}}\right)^{\frac{1}{3}}\left(\bar{k}\bar{\rho}\bar{C}_p\right)^{\frac{1}{2}} \qquad 6.25$$

where all the quantities now refer to the three-phase suspension and are computed according to the following relation listed in [51]:

$$\bar{\rho} = v_s\,\rho_s + v_L\,\rho_L \qquad 6.26$$

$$\bar{\mu} = \mu_L (1 + 4.5 v_s) \qquad 6.27$$

$$\bar{k} = k_L \frac{2k_L + k_s - 2v_s(k_L - k_s)}{2k_L + k_s - v_s(k_L - k_s)} \qquad 6.28$$

$$\bar{C}_p = w_s C_{ps} + w_L C_{pL} \qquad 6.29$$

Following the reasoning given by Deckwer [93] for heat transfer from an immersed surface to liquid agitated by gas in a bubble column, Deckwer et al. [51] have proposed that the heat transfer coefficient from an immersed surface to a three-phase dispersion may be given by the following relation:

$$St = 0.1\left[Re\ Fr\ Pr^2\right]^{-0.25} \qquad 6.12$$

This expression is valid for gas velocities up to 10 cm/s and thereafter h_w asssumes a constant value. Here

$$St = h_w/\bar{\rho}\,\bar{C}_p\,U_g \qquad 6.30$$

$$Re = U_g\ d_p\,\bar{\rho}/\bar{\mu} \qquad 6.31$$

$$Fr = U_g^2/gd_p \qquad 6.32$$

and

$$Pr = \bar{C}_p\,\bar{\mu}/\bar{k} \qquad 6.33$$

$\bar{\rho}$, $\bar{\mu}$, $\bar{k}$ and $\bar{C}_p$ in the above equations are as defined by relations of Eqs. (6.26) - (6.29).

Pandit and Joshi [106] while reviewing the heat transfer literature in three-phase gas sparged reactors have mentioned that the difference between heat transfer coefficient for small particles (<100 μm) for gas-liquid and gas-liquid-solid systems is nominal. However, this difference was found to increase with an increase in the solid-phase holdup. h_w increases with d_p and levels off for d_p greater than 3mm. A maximum value of h_w occurred at a specific value of ϵ_s. This value of ϵ_s depends upon the value of d_p. h_w is found to be practically independent of the value of column diameter. They [106] also remarked that the h_w value is the same for the column wall and for a surface immersed in the reactor.

For the case of small particles (<100μm) and in the absence of liquid flow, Pandit and Joshi [106] have proposed the following explicit relation for the estimation of h_w:

$$h_w = 0.087\,(U_g - \epsilon_g U_{b\infty})^{0.266}\, g^{0.26}\, \bar{\rho}^{\,0.8}\, \bar{C}_p^{\,0.34}\, \bar{\mu}^{-0.33}\, \bar{k}^{\,0.66}\, D_T^{0.06}\, \mu_w^{-0.14} \qquad 6.34$$

Here h_w = 0.087 in kcal/m^2$\cdot$C h, U_g is in m/s, ϵ_g is fractional gas holdup, $U_{b\infty}$ is the terminal rise velocity of a single bubble in m/s, g is the acceleration due to gravity in m^2/s, $\bar{\rho}$ defined by Eq. (6.26) is in kg/m^3, $\bar{C}_p$ defined by Eq. (6.29) is in k cal/kg.°C, $\bar{\mu}$ defined by Eq. (6.27) in kg/m s, $\bar{k}$ defined by Eq. (6.28) is in kcal/m°C s, D_T is the column diameter in m, and μ_w is the viscosity of water in kg/m s. The gas-phase holdup was correlated by an equation of the following type.

$$\epsilon_g = \frac{U_g}{a + bU_g} \qquad 6.35$$

for each value of ϵ_s. The constant a was identified with $U_{b\infty}$. They have prepared a table listing the constants a and b as a function of particle diameter and solid-phase holdup.

Kim et al. [107] have synthesized the data of two-phase (liquid-solid) and three-phase fluidized-bed heat transfer on the basis of the following correlation which implies the heat transfer model of the surface renewal type with isotropic turbulence.

$$h_w = 0.0722\left(k_L \rho_L C_{pL}\left\{\left[(U_L + U_g)\left(\epsilon_g \rho_g + \epsilon_L \rho_L + \epsilon_s \rho_s\right) - U_L \rho_L\right] g (\epsilon_L \mu_L)^{-1}\right\}^{\frac{1}{2}}\right)^{\frac{1}{2}} \qquad 6.36$$

For a slurry bubble column with $U_L = 0$, the above relation reduces to:

$$h_w = 0.0722\left(k_L \rho_L C_{pL} \left\{ \left[U_g\left(\epsilon_g \rho_g + \epsilon_L \rho_L + \epsilon_s \rho_s\right)\right] g (\epsilon_L \mu_L)^{-1} \right\}^{\frac{1}{2}}\right)^{\frac{1}{2}} \qquad 6.37$$

Deckwer et al. [51, 93] relation of Eq. (6.12) as applied to two-phase (gas-liquid) bubble column can be rearranged to obtain the following explicit relation for the heat transfer coefficient:

$$h_w = 0.1 \left[(k_L \rho_L C_{pL}) (P_v/\mu_L)^{\frac{1}{2}}\right]^{\frac{1}{2}} \qquad 6.38$$

where energy dissipation per unit volume, p_v, is,

$$P_v = g U_g \rho_L \qquad 6.39$$

Suh et al. [108] have derived a similar relation for liquid fluidized beds and proposed the following relation for the energy dissipation term for three-phase fluidized beds:

$$P_v = \left[(U_L + U_g)\left(\epsilon_s \rho_s + \epsilon_L \rho_L + \epsilon_g \rho_g\right) - U_L \rho_L\right] g/\epsilon_L \qquad 6.40$$

Kim et al. [107] in deriving Eq. (6.37) have used the relation of Eq. (6.40). Suh et al. [108] proposed a numerical coefficient of 0.0647 in Eq. (6.37) instead of 0.0722. A recent analysis of Suh and Deckwer [109] shows that the form of Eq. (6.38) with p_v given by Eq. (6.40) is appropriate for slurry bubble columns as well as for three-phase fluidized beds with Newtonian and non-Newtonian fluids. For bubble columns with $U_L = 0$, the expression of Eq. (6.40) for p_v is simplified to

$$P_v = \left[U_g\left(\epsilon_s \rho_s + \epsilon_L \rho_L + \epsilon_g \rho_g\right)\right] g/\epsilon_L \qquad 6.41$$

Combining Eqs. (6.38) and (6.41), we get the h_w equation of Suh and Deckwer [109] for a slurry bubble column as follows:

$$h_w = 0.1\left(k_L \rho_L C_{pL} \left\{ \left[U_g\left(\epsilon_s \rho_s + \epsilon_L \rho_L + \epsilon_g \rho_g\right)\right] g (\epsilon_L \mu_L)^{-1} \right\}^{\frac{1}{2}}\right)^{\frac{1}{2}} \qquad 6.42$$

Suh and Deckwer [109] also proposed that μ_L in Eqs. (6.38) and (6.42) represented the apparent effective bed viscosity (μ_b), and for the case of three-phase systems in Eq. (6.42) μ_L be replaced by μ_b. They [109] further suggested that μ_b be computed by the theoretical expression derived by Vand [52], Eq. (4.4). Equation (6.42) is indeed similar to Eq. (6.37) except for the numerical constant and m_b instead of μ_L.

Kato et al. [110] have reported values of heat transfer coefficient between the column wall and fluidized beds of air-water-glass beads. The fluidized beds used were 5.2 and 12.0 cm internal diameter transparent acrylic columns and glass beads of diameter 420 μm, 660 μm, 1.2 mm and 2.2 mm. The heat transfer section for the 5.2 cm column consisted of a 3 cm long and 2 mm thick copper pipe, while for the 12.0 cm column it was 10 cm long and 1 mm thick copper pipe. The heater section was located 25 cm above the distributor and sheath nichrome wire was wound around the outer surface of the pipe. The heat flux through the copper surface was calculated from the power consumption of the electric heater. The temperature difference between the heat transfer surface and the fluidized bed was 0.8 - 3 K. The temperature of the heat transfer surface was maintained close to the ambient temperature and the temperature at the entrance of the bed was 283-301 K, and was kept constant during the experiment to + 0.12 K. The water velocity was varied in the range 0.3 to 10 cm/s while the air velocity was chosen at 2.0 and 10 cm/s.

In the 0.12 m internal diameter column, the influence of gas velocity, liquid velocity and particle size on heat transfer coefficient for gas-liquid-solid fluidized beds was investigated. With increasing liquid velocity, the heat transfer coefficient initially increased, passed through a maximum and a minimum, increased rapidly, and then the degree of the increase in heat transfer coefficient decreased with further increase in liquid velocity. In this region, the flow state of the gas-liquid-solid fluidized bed was stable. The liquid velocity at which the bed became stable was represented by $\overline{U}_{13}$. The small of $\overline{U}_{13}$ increased with increasing particle size and gas velocity for small particles, but it was hardly influenced by gas velocity for large particles.

The heat transfer coefficient for liquid velocities greater than $\overline{U}_{13}$ was influenced by the gas flow velocities. The influence was significant at lower liquid velocities as the gas flow induced a significant contribution by creating an internal circulation of liquid flow. The data were correlated by the following relation:

$$Nu' = 0.044\,(Re'\,Pr)^{0.78} + 2.0\,Fr^{0.17} \tag{6.43}$$

Here

$$Nu' = h_w d_p \epsilon_L / k_L (1-\epsilon_L) \tag{6.44}$$

$$Re' = \rho_L U_L d_p / \mu_L (1-\epsilon_L) \tag{6.45}$$

$$Pr = C_{pL} \mu_L / k_L \tag{6.46}$$

and Fr is defined by Eq. (6.32). For zero superficial liquid velocity, the above relation simplifies to the following:

$$Nu' = 2.0\,Fr^{0.17} \tag{6.47}$$

or

$$h_w = \frac{2.0 k_L (1-\epsilon_L)\, U_g^{0.34}}{\epsilon_L d_p^{1.17}\, g^{0.17}} \tag{6.48}$$

The relation of Eq. (6.48) will be examined for its appropriateness in representing our heat transfer data for slurry bubble column with zero liquid flow velocity. It can be seen a priori that Eq. (6.48) will not be very appropriate for reproducing the experimental data in view of its pronounced dependence on d_p while experimentally determined h_w values are almost independent of d_p.

6.3 Comparison of Present Two-Phase Data with Theory: Air-Water System

Our extensive heat transfer data for the air-water system as obtained in the smaller column with a single probe [67 - 69] are discussed [83] and the same are reported in the previous section 6.1. Saxena and Patel [80] have taken similar data for the seven-tube bundle and these values are systematically greater than single tube values, Fig. 4.23. The analysis presented in section 6.2. clearly demonstrated the inability of the existing correlations to reproduce these experimental data. Our analysis revealed that power and semi-logarithmic functions can correlate the data satisfactorily. Figure 6.3 presents this analysis with the following explicit expressions for the two functions.

$$h_w = 10{,}050\ U_g^{0.28} \tag{6.49}$$

and

$$h_w = 7{,}710 + 1.10 \ln U_g \tag{6.50}$$

Heat transfer coefficient taken in the larger column with a single probe [116] are displayed in Fig. 6.4, set g. These are compared with five different correlations as a function of air velocity. In general, the agreement between the experimental (curve g) and theoretical values (curves a-f) is poor in as much as neither the qualitative nor the quantitative dependence of h_w on air velocity is accurately reproduced. The predicted values based on correlations of Fair et al. [85] and Hikita et al. [87], shown as curves a and b respectively in Figure 6.4, under- and over-estimate the experimental data respectively. It would be very useful to develop an accurate correlation which could reproduce the characteristic variation of experimental h_w, viz. a rapid increase in h_w values at lower values of U_g and approaching a constant value at higher values of U_g.

The curve c based on Deckwer's model [93] and strictly valid for values of U_g up to 10 cm/s only, gives a poor reproduction of experimental data. The latter values are consistently underestimated and the model does not have even the qualitative feature of the variation of h_w with U_g. Joshi and Sharma [97] have proposed a circulation cell model, and Joshi et al. [98] have presented two correlations based on analogies with mechanically agitated contactors and with flow pipes. Predictions based on these two correlations are shown as curves d and e respectively in Figure 6.4. In these computations $V_{b\infty}$ is taken as 0.23 m/s following Joshi and Sharma [117] which is based on bubbles of diameters in the

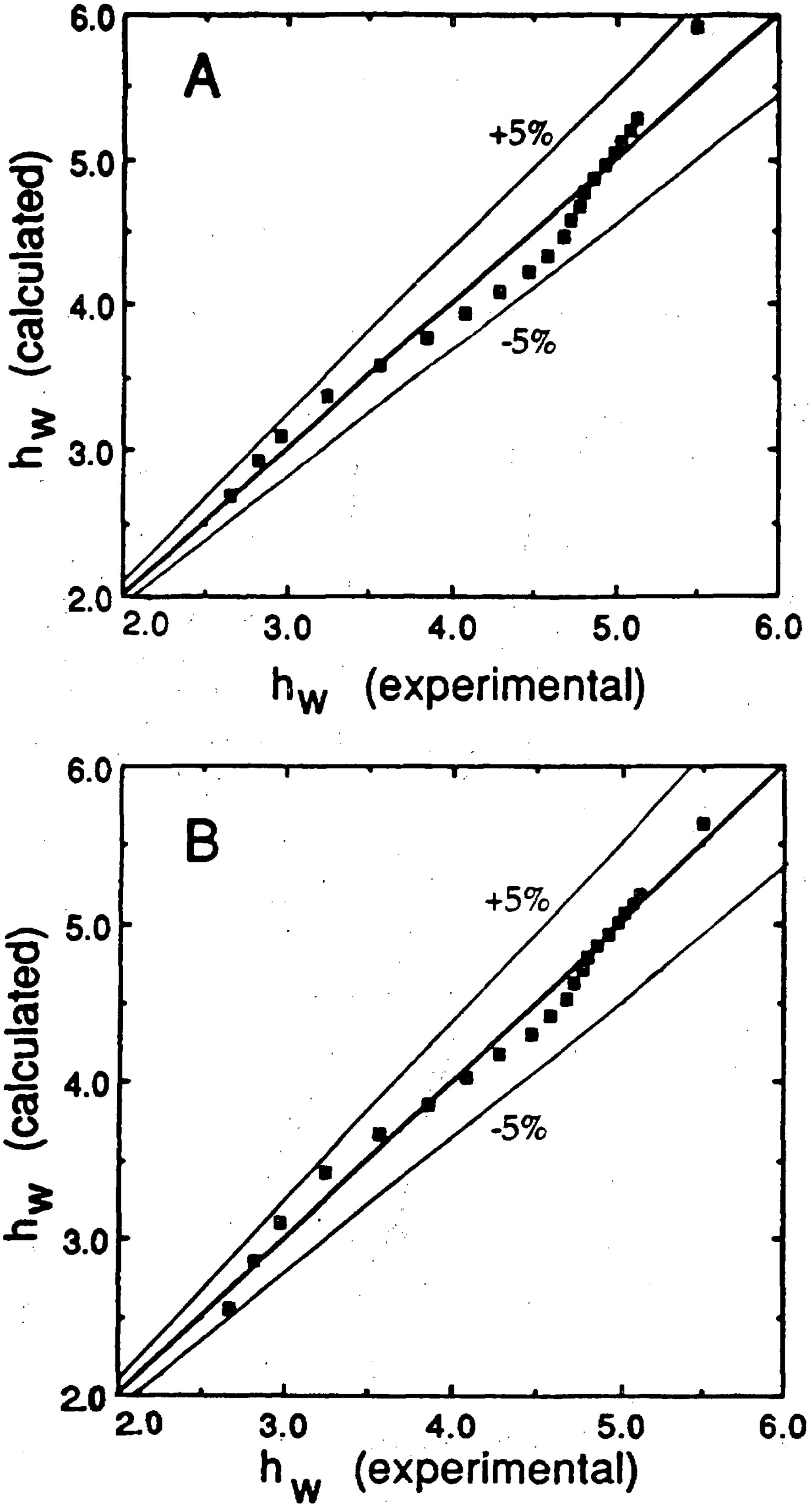

Fig. 6.3. Parity plot of h_W (kW/m^{2}K) for air-water system: (A) power function and (B) logarithmic function.

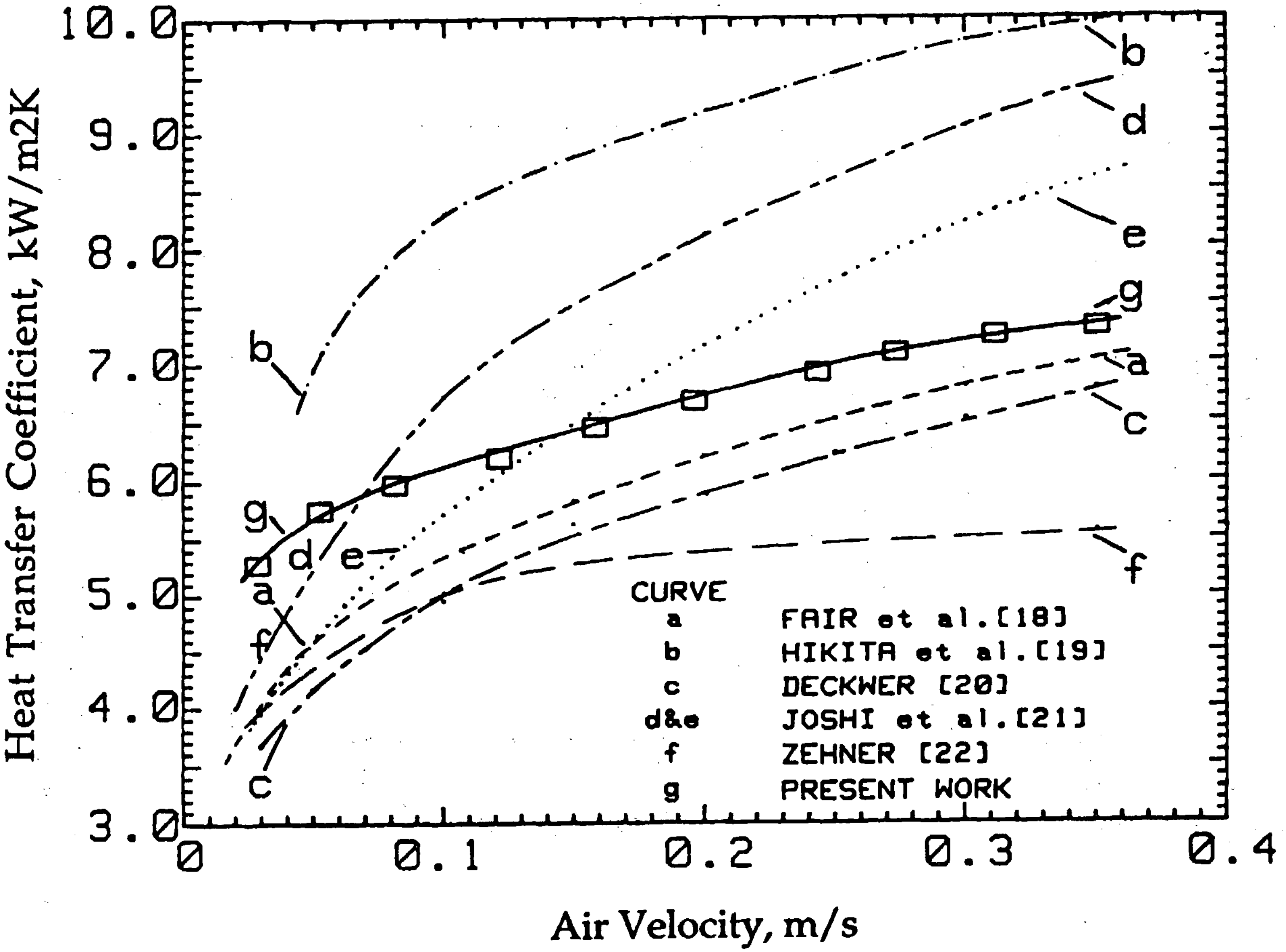

Fig. 6.4. Comparison of the variation of heat transfer coefficient as observed in the larger column for the air-water system at 297K with the predictions of the available correlations and models as a function of air velocity.

range 6 to 7.2 mm and U_g in the range 0.05 to 0.30 m/s. ϵ_g is estimated from the relation developed by Mashelkar [118] for the air-water system. Both sets of values fail to reproduce the experimental data satisfactorily. The set f values are based on the model of Zehner [92, 119] wherein a constant value of 7 mm is assumed for the length of the boundary layer, l. Zehner [92] proposed to use his correlation only up to about 0.1m/s and assumed h_w to be constant thereafter. This model also poorly reproduces the experimental results and the difference between the two sets of values is considerable.

The heat transfer measured with the seven-tube bundle in the larger column [111] at several temperatures are compared with the predictions of relatively successful correlations due to Hakita et al. [87], Pandit and Joshi [106], Kim et al. [107], and Suh and Deckwer [109] in Figure 6.5. The computations performed at the two extreme temperatures, 297 and 343 K, are shown in Figure 6.5, to avoid over crowding. The computed values based on Hikita et al. [87] correlation lead to values which are in poor qualitative agreement with the experimental data. The calculated values of heat transfer coefficient, while smaller than the experimental values at the lower temperature. The Pandit and Joshi [106] correlation based values are considerably smaller than the experimental values at the higher temperatures over the entire air velocity range. On the other hand, at the lower temperature, the computed values are smaller than the experimental values at low air velocities and this trend reverses with the increase in air velocity. In general, the correlation would appear to be inadequate. The Kim et al. [107] correlation predicts values which are consistently smaller than the experimental values, and the disagreement seems to increase rapidly with increase in temperature. The qualitative shape of the dependence of heat transfer coefficient on air velocity is adequately reproduced. However, this correlation will need substantial refinement before reliable predictions may be possible. One such effort was made by Suh and Deckwer [109]. This did improve the agreement between theory and experiment but still the differences are large enough to warrant further refinement of theory. We think this will be in order as some more data on different systems become available.

Zehner [92, 119] proposed a heat transfer model for two-phase systems in the discrete bubbling regime and computed values of heat transfer coefficient from

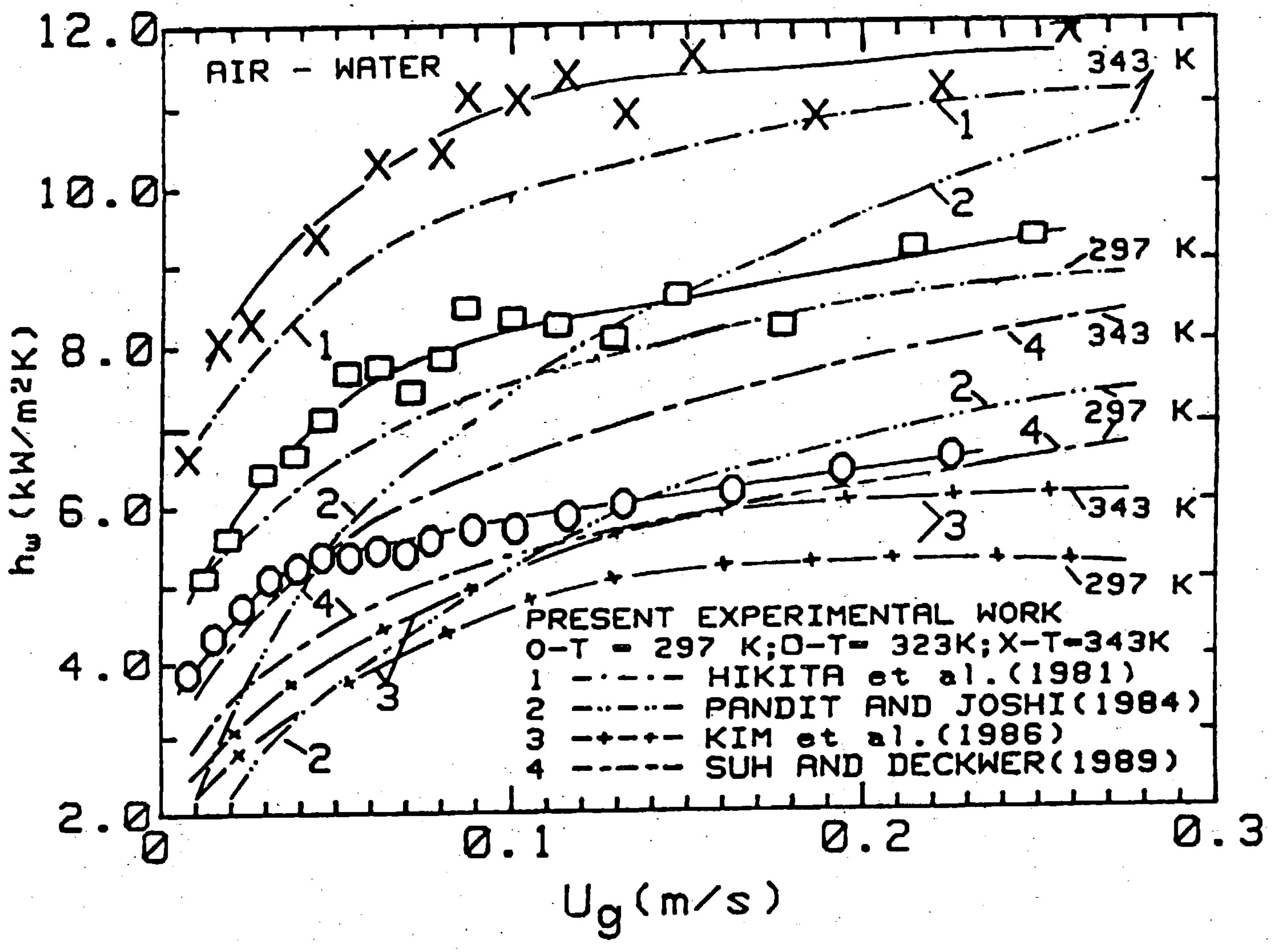

Fig. 6.5. Dependence of heat transfer coefficient for the air-water system on air velocity and temperature. Comparison of experimental data with the predictions of different correlations.

his expressions for the data of Fig. 6.5 are much smaller than the experimental values. At 303 K, the values range between 0.578 to 4.13 kW/m^{2}K for the air velocity range of 0.01 to 0.30 m/s. For the same air velocity range at 343 K, the values range between 0.765 to 5.47 kW/m^{2}K. Thus, the predicted values are an order of magnitude smaller at low air velocities and are about half as large at the highest air velocity. One would have expected a better agreement at lower air velocities and the agreement to deteriorate as the air velocity increases due to bubble coalescence and increasing turbulence.

The Mersmann [103] correlation developed for the maximum heat transfer coefficient in analogy to the phenomenon of free convection predicts values in this temperature range which vary from 4.22 to 4.87 kW/m^{2}K. These values are somewhat smaller than our experimental values and the difference increases as the temperature increases. This conclusion is in agreement with our [83] earlier finding at ambient temperature in Figure 6.1.

It may be recalled that h_w data for single, five and seven-tubes do not differ much from each other as also evident from the data plotted in Figure 4.63. This is understandable because the tubes occupy only a small fraction of the column in the center. This will not be the case for the thirty-seven tube bundle where the baffling is appreciable and is uniform throughout the column cross-section. In Figure 6.6A, these h_W data are displayed at 25° C where values for the thirty-seven tube bundle are different and more importantly exhibit a different dependence on air velocity. A similar trend in general is evident at a higher temperature shown in Figure 6.6B at 70°C. It appears that increasing temperature bring about relatively more pronounced changes in h_w as compared to ambient temperature operation. In contrast to gas holdup, heat transfer coefficient is influenced more by the liquid mixing and liquid circulation patterns established by bubbles as the bubble diameter decreases with increase in the number of tubes in the column. Small bubbles inhibit liquid circulation to some extent in a well baffled bubble column.

In Fig. 6.7 the heat transfer for air-water (probe 3) are compared with the predictions of Kim et al. [107], Deckwer [93], Suh and Deckwer [109], and Pandit and Joshi [106]. These data are reported in greater detail in Fig. 4.72A and Fig. 4.74. The models poorly estimate the data and always underpredict the

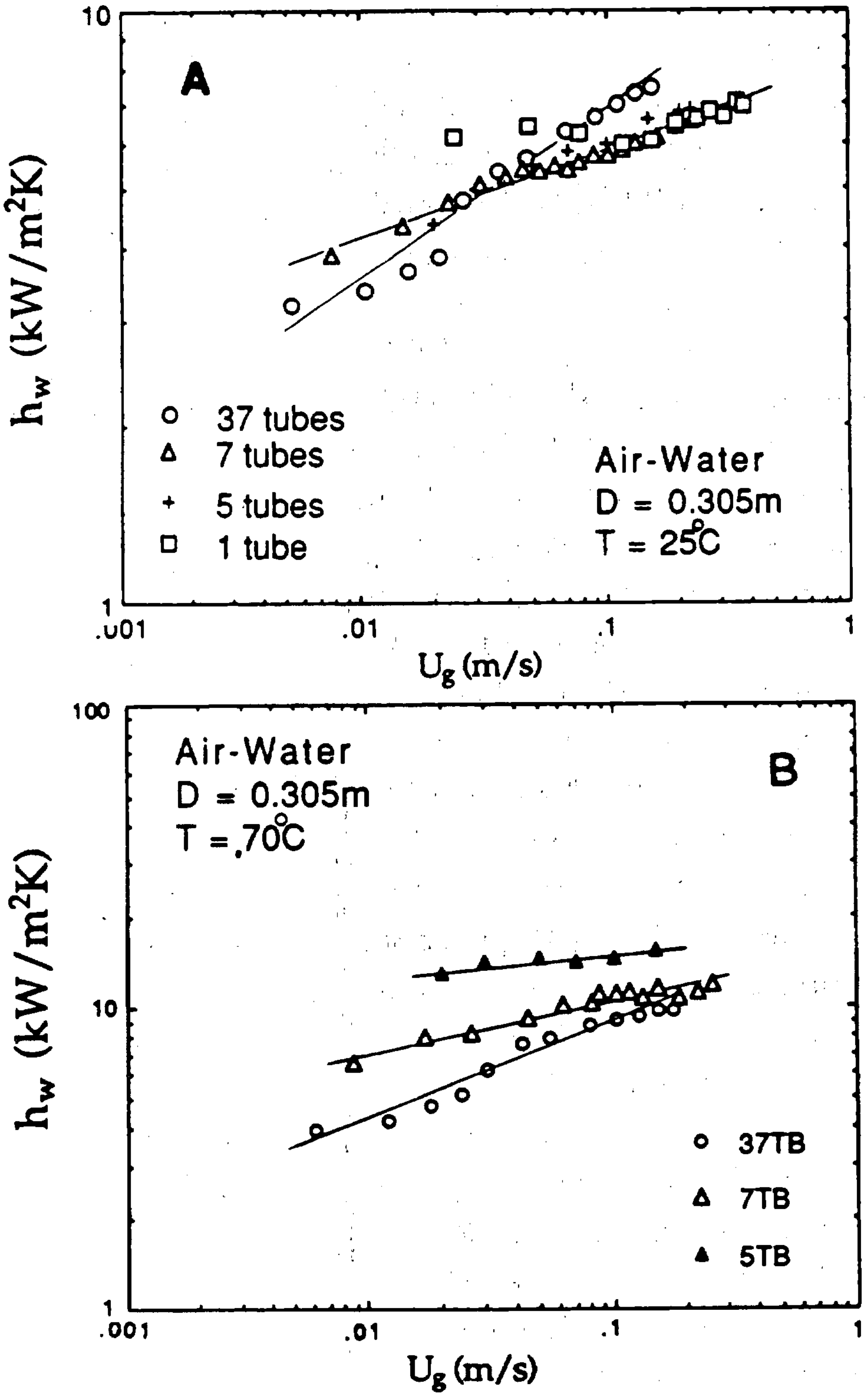

Fig. 6.6. Comparison of h_W for a bubble column equipped with tube bundles of different sizes.

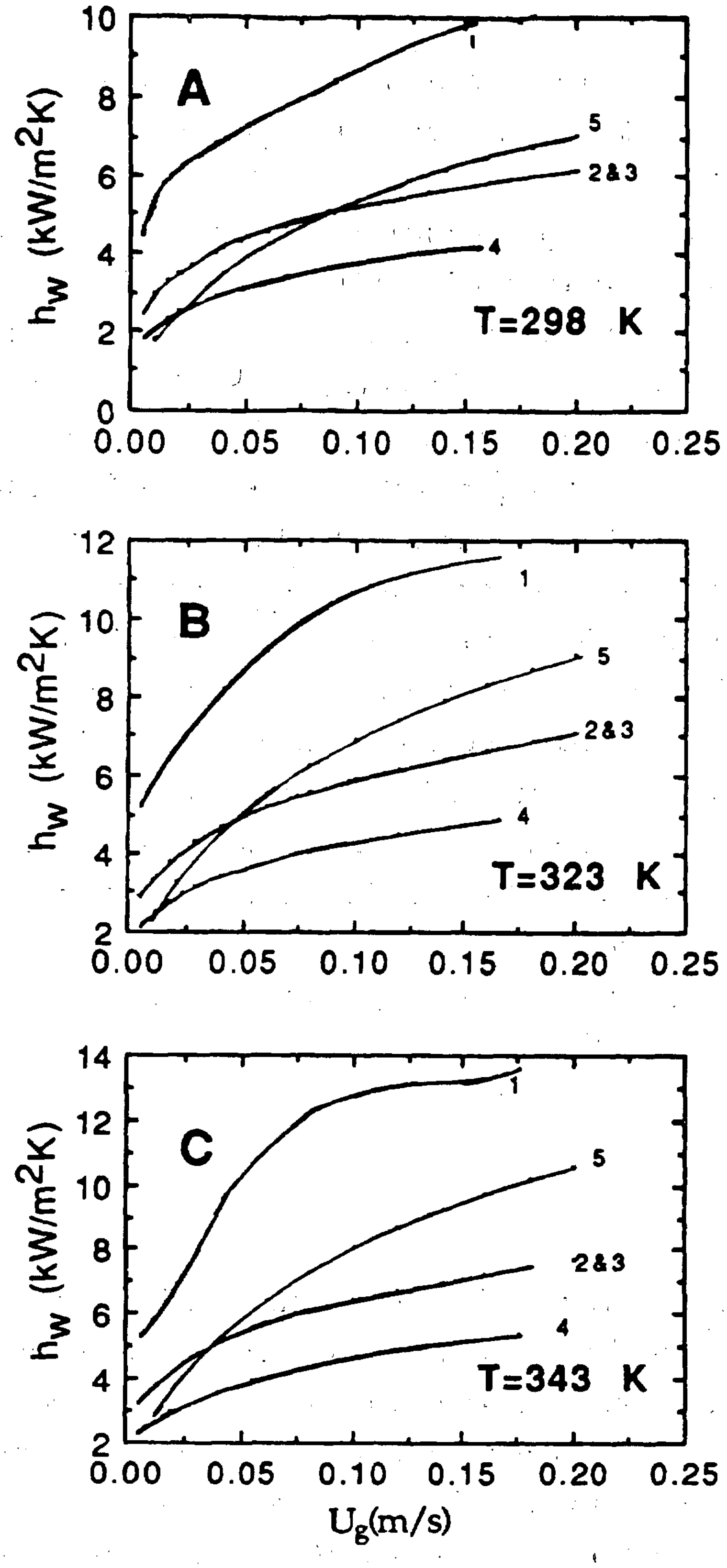

Fig. 6.7. Comparison of experimental heat transfer coefficient data (probe 3) of air-water system with the predictions of different models at four temperatures. (1-Experimental, 2-Deckwer, 3-Suh and Deckwer, 4-Kim et al., 5-Pandit and Joshi).

experimental values. This failure of theory is in conformity with the seven-tube bundle data. These heat transfer data are correlated with a power function in U_g with the results reported in Fig. 6.8.

In Fig. 6.9A the h_w data for 19 mm probe, reported in Fig. 4.38, are compared with the predictions of theoretical expressions due to Deckwer et al. [51], Suh and Decker [109], Kim et al. [107], and Pandit and Joshi [106]. The theoretical expressions of Deckwer et al. [51] and Suh and Deckwer [109] are identical for two-phase systems and hence curves 1 and 2 are the same in Fig. 6.9A. However, these models [51, 109] overestimate the experimental data while models of Kim et al. [107] and Pandit and Joshi [106] underestimate the data. The departure of theoretical curves for the three-phase system (treated here as an effectively two-phase system) from the experimental data are presented in Fig. 6.9 B and these are similar to those found for the two-phase system in Fig. 6.9 A. The Suh and Deckwer [109] correlation based values reproduce the data satisfactorily. This, however, is to be regarded as somewhat fortuitous as this model fails in Fig. 6.9 A. Hence , the need to develop a reliable heat transfer model is obvious. In this context an empirical approach is adopted here following Saxena et al. [120] and is briefly discussed in the following.

The 19 mm heat transfer probe data up to U_g = 0.15 m/s are fitted to an empirical relation of the following type

$$h_w = aU_g^b \tag{6.51}$$

for nitrogen-Therminol system. This yielded a = 1.204 and b = 0.316. Similarly, the three-phase system data for slurry concentrations of 15, 30 and 50 weight percent could be represented by Eq. (6.51) except a and b values are different for each set. Figure 6.10 presents a comparison of these four sets of experimental values with corresponding computed values. One set of a and b values could not represent the entire data for the four sets. This for such fine powder slurries as discussed earlier [120] is due to the changing viscosity of the slurry with the changes in slurry concentration. Hence following our earlier approach, we correlated the data for the four sets by the following relation:

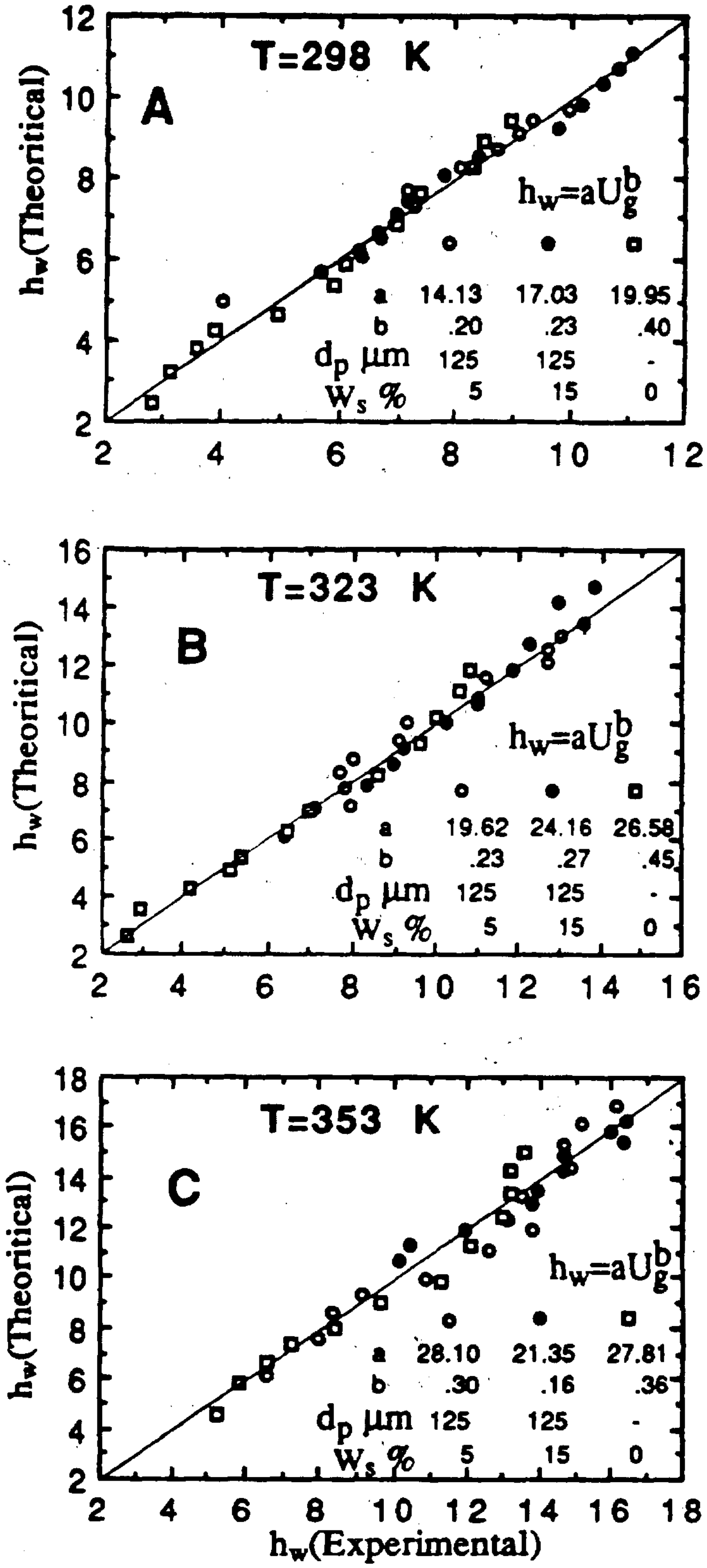

Fig. 6.8. Comparison of experimental heat transfer coefficient data for probe 3 with the predictions of the proposed semi-empirical correlation.

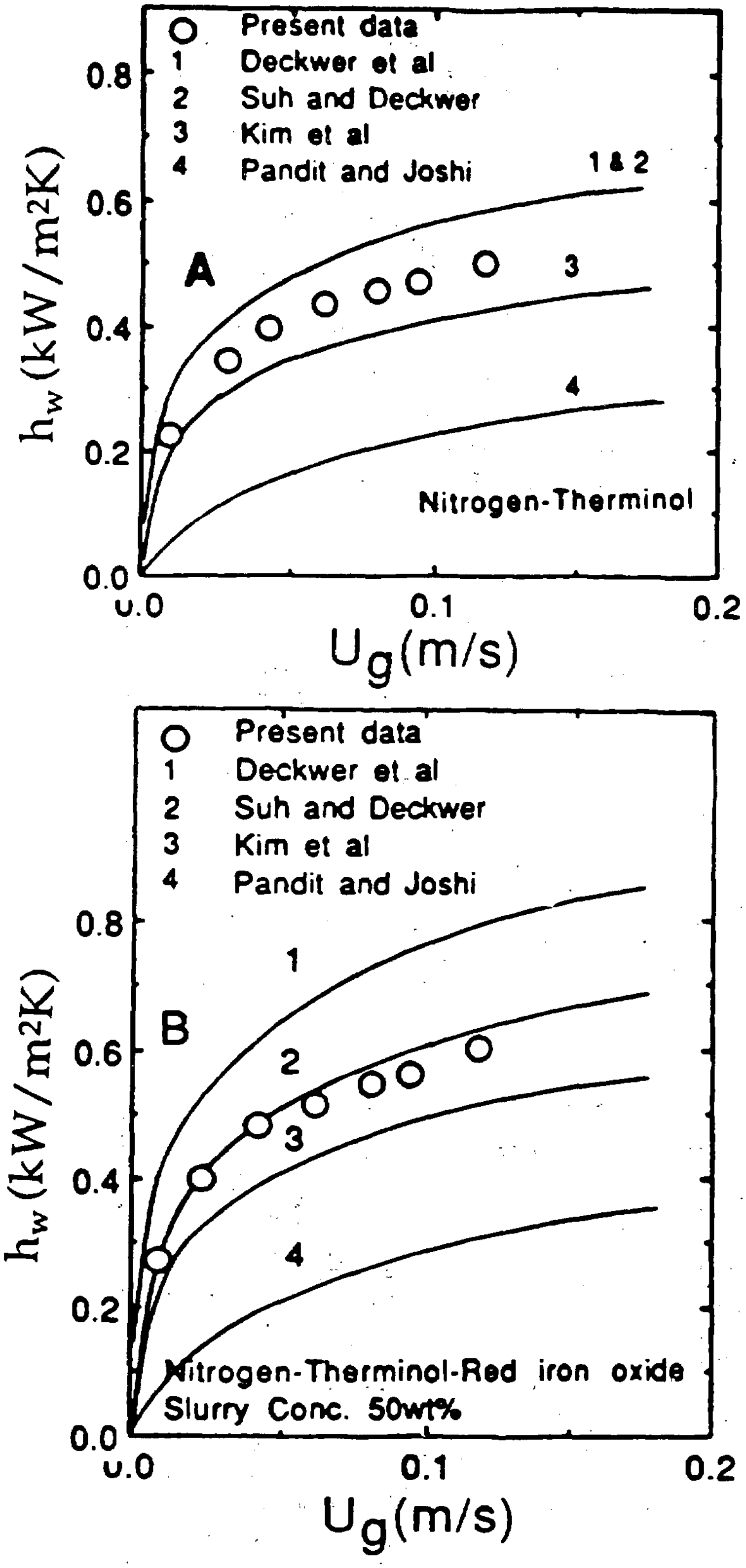

Fig. 6.9. Comparison of experimental h_W data for the 19 mm probe internal with the predictions of different correlations.

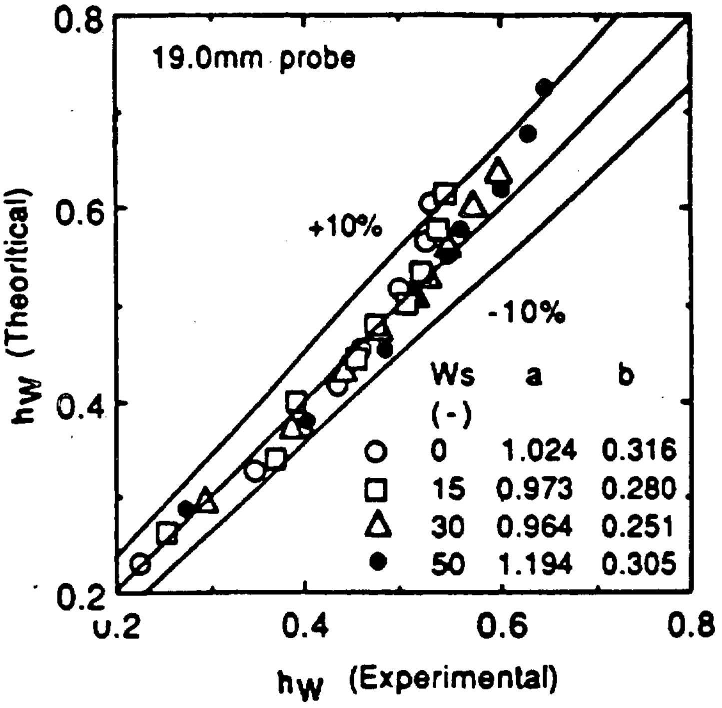

Fig. 6.10. Comparison of experimental h_W data for 19 mm probe internal with the predictions based on Eq. (6.51).

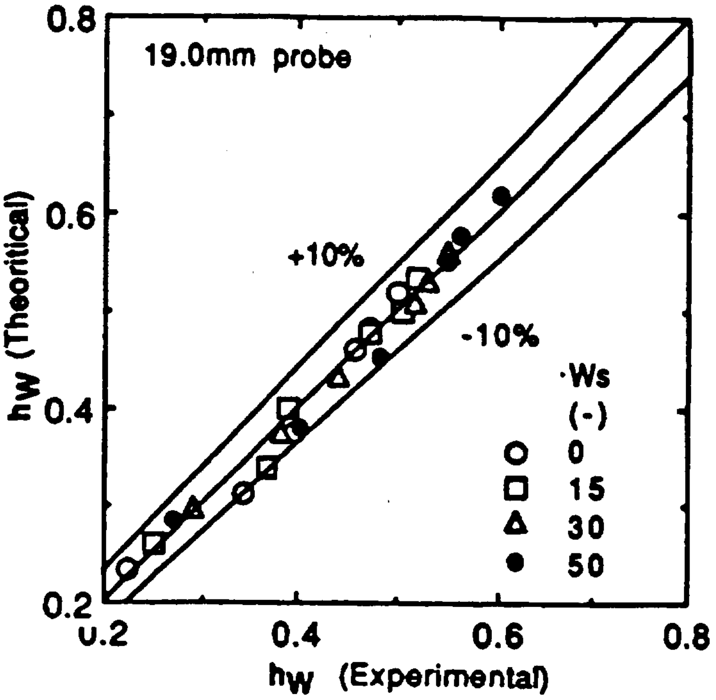

Fig. 6.11. Comparison of h_W for 19mm probe internal with those based on Eq. (6.52).